Proton Transfer in Gramicidin Channels is Modulated by the Thickness of Monoglyceride Bilayers

Anatoly Chernyshev, Kathryn M. Armstrong, and Samuel Cukierman
Department of Physiology, Loyola University Medical Center, Maywood, Illinois 60153

ABSTRACT The thickness of monoglyceride planar bilayers has significant effects on the transfer of protons in both native gramicidin A (gA) and in covalently linked SS- and RR-dioxolane-linked gA proteins. Planar bilayers with various thicknesses were formed from an appropriate combination of monoglyceride with various fatty acid lengths and solvent. Bilayer thicknesses ranged from 25 Å (monoolein in squalene) to 54 Å (monoeicosenoin in decane). Single-channel conductances to protons (g_H) were measured in the concentration range of 10–5000 mM HCl. In native gA as well as in RR channels, the shape of the log(g_H)-log([H^+]) relationships was nonlinear and remained basically unaltered in monoglyceride bilayers with various thicknesses. For both native gA and RR channels, g_H values were systematically and significantly larger in thin than in thick bilayers. By contrast, the shape of the log(g_H)-log([H^+]) relationships in the SS channel was linear (with a slope considerably smaller than 1) in thick (>37 Å) bilayers. However, in thin (<37 Å) bilayers these plots became nonlinear and g_H values approached those obtained in native gA channels. The linearization of the log-log plots in the SS channel in thick bilayers is a consequence of a dramatic increase (instead of a decrease as in native gA and RR channels) of g_H in these bilayers in [H^+] <1 M. The gating characteristics of the various gA channels as a function of bilayer thickness followed the same pattern as described previously. It was noticed, however, that in the thickest monoglyceride bilayer used in this study, both the SS- and RR-dioxolane-linked channels opened in a mode of bursting activity instead of remaining in the open state as in thin bilayers. It is proposed that the thickness of monoglyceride bilayers modulates proton transfer in native gA channels by a combination of factors including the access resistances of channels to H^+, and fluctuations in both the structure of the lipid bilayer and in the distance between gA monomers. The differential effects of relatively thick monoglyceride bilayers on proton transfer in both dioxolane-linked gA channels must relate to distinct interactions between the bilayers and the SS and RR dioxolanes.

INTRODUCTION

The conductivity or mobility of protons in water is considerably larger than that of any other ion. In relatively dilute acid solutions, protons do not diffuse hydrodynamically but by a specific mechanism that became known as Grotthuss's mechanism. In this mechanism, protons are transferred between adjacent water molecules as a consequence of a dynamical reorganization of both the covalent bonds in water molecules, and the H-bonds between water molecules (Agmon, 1996; Bernal and Fowler, 1933; Conway et al., 1956; Cukierman, 2000; Day et al., 2000; Danneel, 1905; DeCoursey and Cherny, 1994; Phillips et al., 1999; Pomès and Roux, 1996, 1998). The classical Grotthuss's mechanism (see below) is of interest to a particular configuration of water molecules known as water or proton wires (Nagle and Morowitz, 1978; Nagle and Tristam-Nagle, 1983). In proton wires, H-bonded water molecules are arranged in a single file, and protons can be transferred between water molecules by hop and turn steps (Grotthuss's mechanism). The approach of a proton to an oxygen of a water molecule leads to the formation of a new covalent bond between these atoms. As a consequence, one of the protons that was initially covalently linked to the oxygen of that water molecule will be shared with an adjacent water forming a protonated water dimer $(H_5O_2)^+$. This hopping step propagates between adjacent water molecules in the proton wire. As the proton hops the dipole moment of the water donating the proton is reversed. Once the proton leaves the wire, the total dipole movement of the water wire is reversed. If another proton must be transferred in the same direction as before, waters need to rotate back to their original configurations (for a more detailed explanation and illustrations, see, for example, Godoy and Cukierman, 2001; Phillips et al., 1999; Pomès and Roux, 1996). The turn step is considered the rate-limiting step for proton transfer in water wires in computational models (Pomès and Roux, 1996, 1998). Less clear, however, is whether the turn step is actually limiting the transfer of protons across membrane proteins.

Unidimensional chains of water molecules have been found in restricted spaces in various proteins that participate in bioenergetic processes (Baciou and Michel, 1995; Branden et al., 2001; Luecke et al., 1999; Sass et al., 2000; Zaslavsky and Gennis, 1998). In virtually all cells, the production of ATP is ultimately triggered by the movement of protons across a membrane protein. The complexity of those proteins associated with a tight functional coupling between proton transfer and redox potentials (Trumpower and Gennis, 1994), and the fact that proton transfer cannot be directly measured in a single molecule, makes it extremely difficult to analyze the fine features of proton transfer in bioenergetic proteins. On the other hand, proton transfer in a relatively simple structure such as gramicidin A (gA)

Submitted July 1, 2002 and accepted for publication August 29, 2002.

Address reprint requests to Samuel Cukierman, Dept. of Physiology, Loyola University Medical Center, 2160 South First Avenue, Maywood, IL 60153. Tel.: 708-216-9471; Fax: 708-216-6308; E-mail: scukier@lumc.edu.

0006-3495/03/01/238/13 $2.00

channels can be directly measured at the single molecular level, and insights can be gained into the basic rules that govern proton transfer in proteins.

gA is a highly hydrophobic pentadecapeptide secreted by *Bacillus brevis*. In lipid bilayers, its primary structure (HCO-*L*-Val-Gly-*L*-Ala-*D*-Leu-*L*-Ala-*D*-Val-*L*-Val-*D*-Val-(*L*-Trp-*D*-Leu)$_3$-*L*-Trp-NH-(CH$_2$)$_2$-OH) defines a right-hand $\beta^{6.3}$ helix in which the side chain residues are in contact with the lipid environment, and the carbonyl and amide groups line the pore of the protein (Arseniev et al., 1985; Ketchem et al., 1993, 1997; Sarges and Witkopf, 1965; Urry, 1971). The association via six intermolecular H-bonds between the amino termini of two gA peptides, each located in a distinct monolayer, results in the formation of a water-filled ion channel that is selective for monovalent cations (Andersen, 1984; Koeppe and Andersen, 1996; Hladky and Haydon, 1972). Disruption of intermolecular H-bonds results in the dissociation of gA monomers with the consequent loss of ion channel function.

Four distinct and direct experimental evidences support the notion that the single-channel conductance to protons (g_H) in gA channels is determined by proton transfer. *1*) Proton permeation in gA channels is 1–2 orders of magnitude larger than the second most permeable ionic species (Cs^+; Armstrong et al., 2001; Busath and Szabo, 1988; Eisenman et al., 1980; Hladky and Haydon, 1972; Myers and Haydon, 1972; Quigley et al., 2000). *2*) Levitt et al. (1978) and Finkelstein (1987) demonstrated that the permeation of protons through native gA channels is not accompanied by water movement as with other monovalent cations. *3*) The kinetic isotope effect for H^+ transfer in native gA (Akeson and Deamer, 1991), and in both the SS- and RR-dioxolane-linked gA dimers (Chernyshev et al., 2003) is larger than the kinetic isotope effect for other monovalent cations (Tredgold and Jones, 1979), and consistent with a proton transfer mechanism (Chernyshev et al., 2003). *4*) Activation energies for proton transfer in native gA and in the SS- and RR-dioxolane-linked gA dimers (Akeson and Deamer, 1991; Chernyshev and Cukierman, 2002) are in general less than with single-channel conductances to alkalines (Chernyshev and Cukierman, 2002; DeCoursey and Cherny, 1998) and consistent with those of proton transfer in bulk solution (Chernyshev and Cukierman, 2002).

Two desformylated gA peptides have been covalently linked with various chemical groups: malonyl (Bamberg and Janko, 1977; Urry et al., 1971), glutaryl (Rudnev et al., 1981), and the SS and RR diacid dioxolane (Cukierman et al., 1997; Quigley et al., 1999; Stankovic et al., 1989). Those covalently linked gA peptides form ion channels in lipid bilayers with single-channel conductance properties similar to native gA channels. As expected, the average lifetime of covalently linked gA channels is considerably longer than in native gA. In our laboratory, the SS- and RR-dioxolane-linked dimers have been used as experimental models to probe structure–function relationships of proton transfer in proteins (Armstrong et al., 2001; Armstrong and Cukierman, 2002; Chernyshev and Cukierman, 2002; Chernyshev et al., 2003; Cukierman et al., 1997; Cukierman, 1999; 2000; Godoy and Cukierman, 2001; Quigley et al., 1999). One of the most challenging questions that we pose is illustrated in Fig. 1.

The top panel of this figure shows log(g_H)-log([H^+]) for native gA channels (*circles*), and for the SS- (*squares*) and RR- (*triangles*) dioxolane-linked gA dimers (for the sake of brevity, these channels will be referred to as the SS and RR channels). These measurements were obtained in glyceryl-monooleate (GMO)/decane bilayers (Cukierman, 2000). Each of these channels has a typical proton transfer signature. In the SS channel, the log-log relationship between g_H and [H^+] is a straight line with a slope of 0.75 within the concentration range of 0.001−~2 M. The bottom panel

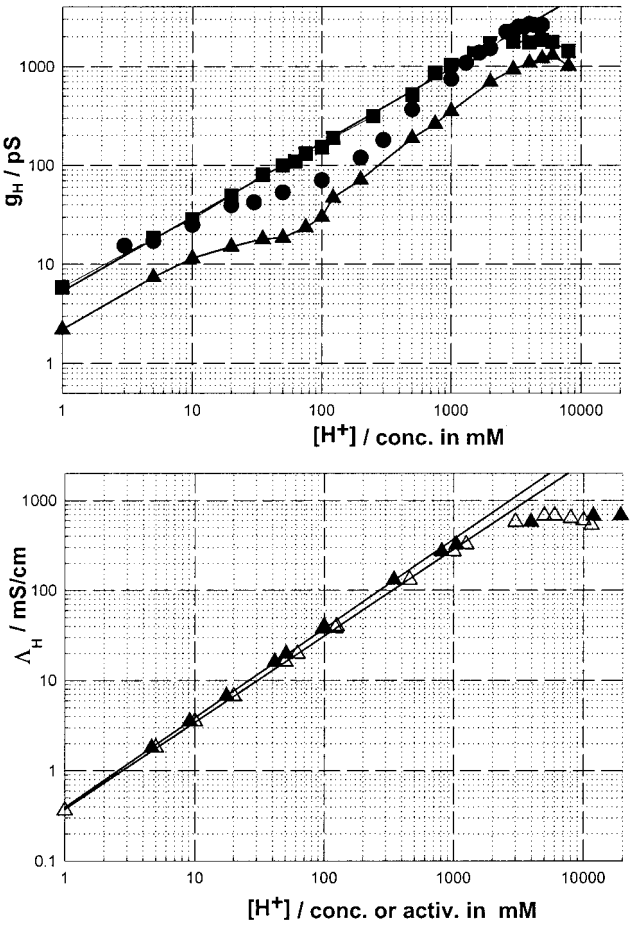

FIGURE 1 The top panel shows log-log plots of g_H vs. [H^+] for the SS (*squares*), RR (*triangles*), and native gA (*circles*) channels in a GM-C_{18}/decane bilayer. The experimental points for the SS and RR channels in this figure are from Cukierman (2000). Those for gA are from Fig. 5 in this article. In the bottom panel, proton conductivities in water were plotted as a function of proton concentrations (*open triangles*) or activities (*solid triangles*, see Cukierman, 2000).

shows that the relationship between proton conductivity in water and $[H^+]$ is a straight line (up to a $[H^+]$ of ~1 M) with a slope of 0.98 if proton concentrations are used or 1.00 if those concentrations are corrected for their thermodynamic activities (Cukierman, 2000). At $[H^+] > 1$–2 M, saturation of proton conductivity ensues. Thus, the straight line of the SS channel in Fig. 1 is not a consequence of diffusion limitation of protons in bulk solution. On the other hand, g_H values in RR channels (*triangles*) are considerably smaller than in the SS and native gA channels at any given concentration, and the shape of the $\log[g_H]$-$\log[H^+]$ relationship is not linear, resembling the one for native gA channels as first described by Eisenman et al. (1980) in GMO/hexadecane bilayers, and recently confirmed by Gowen et al. (2002). The experimental points for gA in Fig. 1 were obtained in GMO/decane bilayers. They also show a similar 'shoulder' type appearance (Eisenman et al., 1980; Gowen et al., 2002). Of special interest for the investigation reported in this study is that in the concentration range of 0.010–1 M $[H^+]$, g_H values in the SS channel were considerably larger than in native gA. Notice that at $[H^+]$ larger than 2 M, g_H saturates in the various gA channels. This suggests that at those high $[H^+]$, g_H is limited by proton diffusion in bulk solution (Cukierman, 2000).

In addressing the molecular origin of the brief closures in various gA channels, Armstrong and Cukierman (2002) demonstrated that in 1 M HCl, g_H in GMO/squalene bilayers was considerably larger than in GMO/decane bilayers for native gA, SS, and RR channels. The significant difference between these bilayers is that a GMO/squalene bilayer is ~50% thinner than a GMO/decane bilayer (see below). This result was intriguing and insightful—intriguing, because previous measurements by various investigators have demonstrated that the single-channel conductances to alkalines were not affected by manipulations of membrane thickness via solvent effects (see below, and Hladky and Haydon, 1972; Kolb and Bamberg, 1977; Rudnev et al., 1981); and insightful, because it offered an opportunity to reinvestigate g_H–$[H^+]$ relationships in bilayers with various thicknesses with the aim of identifying the molecular factors that modulate said relationships.

Our objective in this study was to perform a set of systematic measurements of g_H-$[H^+]$ relationships in native gA, SS, and RR channels in monoglyceride bilayers with various thicknesses. It is now demonstrated that g_H-$[H^+]$ relationships in these various gA channels channel are distinctly modulated by the thickness of lipid bilayers. This modulation is considerably more pronounced and distinct in the SS channel in the $[H^+]$ range of 0.01–1 M, which corresponds to the shoulder region in log-log plots of g_H vs. $[H^+]$ (Eisenman et al., 1980; Gowen et al., 2002). We demonstrate that g_H values in the SS channel in that $[H^+]$ range converge to those of native gA channels in thin bilayers. The shape of g_H-$[H^+]$ relationships in distinct gA channels is determined by lipid-protein interactions.

MATERIALS AND METHODS

Planar lipid bilayers

Planar lipid bilayers were formed on a 0.10–0.15-mm diameter hole in a polysterene partition separating two aqueous compartments. The formation (thinning) of a lipid bilayer was monitored visually and/or by measuring the capacitance of the bilayer. The leak resistance of the planar bilayers used in this study in various HCl solutions was larger than 25 GΩ. It has been shown (see below) that the thickness of monoglyceride bilayers depends on the solvent used to form the bilayer. In this study, the monoglycerides contained *cis*-mono-unsaturated fatty acid chains. The composition of the bilayer will be referred to as GM-C_x/solvent, where x is the number of carbons in the fatty acid chain, and the solvent is decane, hexadecane, or squalene. Monoglycerides were purchased from Nu-Check Prep (Elysian, MN): Monoerucin-GM-C_{22} (Δ 13 *cis*-monodocosenoin), Monoeicosenoin-GM-C_{20} (Δ 11 *cis*-monoeicosenoin), Monoolein-GM-C_{18} (Δ 9 *cis*-monoolein), and Monopalmitolein-GM-C_{16} (Δ 9 *cis*-monopalmitolein). Decane, hexadecane, and squalene were obtained from Sigma (St. Louis, MO), and twice purified in a column containing (from bottom to top) neutral, basic, and acid chromatographic grade alumina (Sigma). This purification step is particularly important for squalene (White, 1978). Planar bilayers were formed from a lipid solution of ~60 mg of monoglyceride in 1 mL of solvent.

The thicknesses of planar bilayers formed by a combination of monoglycerides and solvents were measured by various investigators using several techniques (Benz et al., 1975; Dilger, 1981; Dilger and Benz, 1985; Elliot et al., 1983; Lewis and Engelman, 1983; Requena et al., 1975; Rudnev et al., 1981; White, 1978). Table 1 shows the thicknesses of the bilayers used in this study. The thickness of these planar bilayers is essentially determined by the distribution of solvent in the bilayer core. Relatively long chain alkanes (hexadecane) are mostly distributed between fatty acid chains of the monoglycerides whereas alkanes with shorter chains (decane, for example) partition between the monolayers of the bilayer (McIntosh et al., 1980; Simon et al., 1977). On the other hand, squalene seems to be virtually excluded from the lipid bilayer (White, 1978).

The surface tension (σ) of various glycerides at the air/water interface was measured with the Wilhelmy plate method using a tensiometer (KSV Instruments, Helsinki, Finland). A droplet of lipid solution in chloroform was deposited on the water surface, and 15–20 min were allowed for the chloroform to evaporate completely. These measurements were obtained at room temperature (24°C), and are also reported in Table 1.

Channels

The gA peptides were obtained from Fluka (Milwaukee, WI). The SS and RR stereoisomers of dioxolane-linked gA channels were synthesized, purified, and characterized as previously described (Cukierman et al., 1997; Quigley et al., 1999; Stankovic et al., 1989).

TABLE 1 Hydrocarbon thickness of planar lipid bilayers, and surface tension measurements at air/water interface

	σ[1]	Decane	Hexadecane	Squalene
GM-C_{14}	63.6 ± 4.1	38 Å		
GM-C_{16}	41.3 ± 4.1	42 Å	28 Å	
GM-C_{18}	43.7 ± 0.3	48 Å	32 Å	25 Å[2]
GM-C_{20}	40.6 ± 3.8	54 Å	37 Å	
GM-C_{22}	32.7 ± 2.5		49 Å	

Unless otherwise stated, thickness measurements reported in this Table were from Benz et al. (1975).
[1]In mN/m (mean ±SE of four to six measurements).
[2]Dilger (1981); Dilger and Benz (1985).

Solutions

Most experiments were performed with symmetrical solutions of HCl of various concentrations across the bilayer. Some experiments were also performed in 1 or 0.25 M CsCl. All experiments were performed at room temperature (22–24°C).

Electrical measurements

The planar bilayer was voltage-clamped at voltages where g_H has an ohmic behavior, and single-channel currents were measured using a pair of 0.5 mm Ag/AgCl silver wires immersed in distinct solutions across the lipid bilayer. For a given experimental condition (one gA channel in one type of bilayer in a given solution), at least seven measurements of single channels were obtained from at least two (usually more than four) distinct planar bilayers. Single-channel conductances were measured in sectors of the recording where flickers were absent or occurred at a very low frequency. Single-channel conductances are expressed as mean ± SE.

Analysis

Single-channel recordings were digitized and analyzed using pClamp software (Axon Instruments, Union City, CA). Statistical analysis and graphs were done with Sigmaplot 2000 (SPSS Science, Chicago, IL).

RESULTS

Proton transfer and the thickness of monoglyceride membranes

Fig. 2 shows single-channel recordings of native gA channels in 0.25 M HCl in GM-C_{18}/decane (*top*) and GM-C_{18}/hexadecane (*bottom*) bilayers. g_H values were slightly but consistently larger in GM-C_{18}/hexadecane than in GM-C_{18}/decane bilayers (195 and 214 pS in the top and bottom recordings, respectively). Notice also the typical increased lifetime of the channel in the open state, and the lack of closing flickers in GM-C_{18}/hexadecane bilayers (Armstrong and Cukierman, 2002). By contrast, recordings in similar bilayers and $[H^+]$ with SS channels revealed a major attenuation (instead of a slight enhancement as with gA channels) of g_H in GM-C_{18}/hexadecane as compared to GM-C_{18}/decane bilayers. Typical results are shown in Fig. 3. In this figure, g_H values for the SS channel were 270 and 160 pS in GM-C_{18}/decane, and GM-C_{18}/hexadecane bilayers, respectively. Flickers in the SS channel were also practically absent in GM-C_{18}/hexadecane (Armstrong and Cukierman, 2002). Recordings of single RR channels in the same experimental conditions as in the two previous figures are shown in Fig. 4. As with native gA channels, proton transfer in RR channels is larger in GM-C_{18}/hexadecane bilayers (72 and 90 pS for the top and bottom recordings, respectively).

Most of the experimental observations that will be discussed in this article are summarized in Fig. 5. This figure shows several log-log plots of g_H vs. $[H^+]$ in monoglyceride bilayers with various thicknesses (Table 1).

Let us first concentrate on the open symbols of Fig. 5 (*circles*, native gA channels; *squares*, SS channels) and at

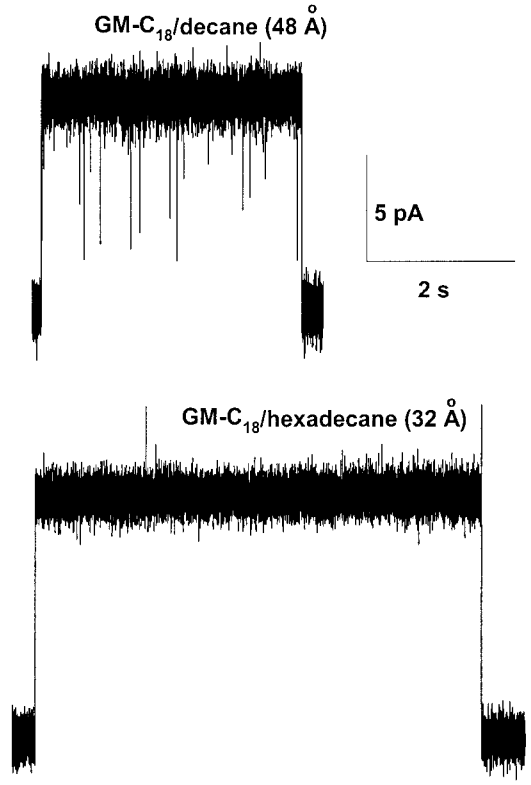

FIGURE 2 Recordings of native gA channels at a transmembrane voltage of 50 mV in 0.25 M $[H^+]$. Recordings were digitally filtered at 2 kHz and digitized at 10 kHz. Channel openings are represented by upward trace deflections.

$[H^+] < 2$ M. In bilayers whose thicknesses were between 54 and 42 Å, the log[g_H]-log[H^+] relationships were linear for the SS channel in $[H^+] \leq 2$ M. Notice that the slopes of these linear relationships are slightly different (0.66–0.85; see Fig. 5 legend) in various bilayers. Perhaps the most interesting experimental finding in this article concerns the fact that in monoglyceride bilayers whose thicknesses are smaller than 37 Å, the relationships between g_H and $[H^+]$ in the SS channel became essentially indistinguishable from those in native gA channels in log–log plots. In the thicker bilayers, log–log relationships became linear in the SS channel.

By contrast, the log(g_H)-log($[H^+]$) relationships for native gA channels display the usual shoulder-like appearance (Eisenman et al., 1980; Gowen et al., 2002) as previously mentioned in the Introduction. This shape was independent of the thickness of monoglyceride bilayers (see also Fig. 7, *top panel*). In thick (>37 Å) monoglyceride bilayers, g_H values in native gA channels at $[H^+] < 1$ M were significantly smaller than in SS channels. At $[H^+] > 1$ M, however, g_H values were larger in native gA channels.

In relatively thin bilayers, g_H values in the SS channel decreased and approached those measured in native gA channels for $[H^+] \leq 1$ M (see Fig. 3). This point is further documented in Fig. 6. In this figure, the ratios between g_H values in GM-C_{18}/decane (48 Å) and GM-C_{18}/hexadecane

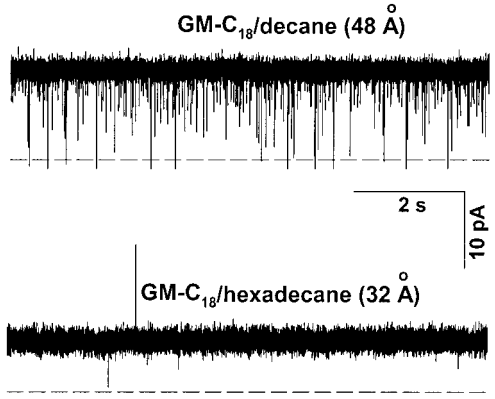

FIGURE 3 Recordings of single SS channels obtained at a transmembrane voltage of 50 mV in 0.25 M $[H^+]$. Recordings were digitally filtered at 2 kHz and digitized at 10 kHz. The dashed line represents the current level at the closed state.

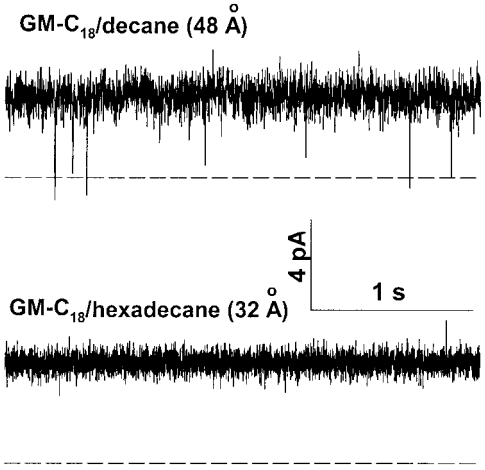

FIGURE 4 Recordings of single RR channels obtained at a transmembrane voltage of 50 mV in 0.25 M $[H^+]$. Recordings were digitally filtered at 500 Hz and digitized at 2 kHz. The dashed line represents the current level at the closed state.

(32 Å) for the SS (*squares*), and native gA (*circles*) and RR channels (*triangles*) were plotted as a function of $[H^+]$. In native gA and RR channels, the ratios between g_H values remained relatively constant or slightly less than 1 at various $[H^+]$ (see Figs. 2, 6, and 8). By contrast, these ratios could be twice as large in the SS channel (see also Fig. 3). Consequently, the convergence between the g_H values of the SS and native gA channels in $[g_H]$-$[H^+]$ plots in thin GM-C_{18}/hexadecane bilayers (*middle panel, right column* of Fig. 4) is a consequence of a major attenuation of g_H in the SS channel in thin bilayers at $[H^+] < 1$ M.

In Fig. 7, the $\log(g_H)$-$\log([H^+])$ plots obtained in various bilayers were superimposed for native gA (*top panel*), SS (*middle panel*), and RR channels (*bottom panel*). In general, at a given $[H^+]$ g_H values did not increase or decrease monotonically as a function of membrane thickness. Also, a given particular sequence of ascending g_H values in bilayers of various thicknesses at a given $[H^+]$ did not necessarily apply to other $[H^+]$. Nevertheless, some strong and general experimental conclusions can be stated:

1. In native gA or RR channels, the maximum g_H values at any given $[H^+]$ (g_H^{max}) were systematically measured in the thinnest bilayers (GM-C_{18}/squalene, ◇; GM-C_{16}/hexadecane, △). By contrast, g_H^{max} values for the SS channel were measured in either GM-C_{18}/decane (●) or GM-C_{16}/decane (▲) bilayers. Notice that for the SS channel, the solid symbols (thick bilayers) in Fig. 7 are consistently larger than the open (thin bilayers) symbols in various $[H^+]$.
2. The minimum g_H values at any given $[H^+]$ (g_H^{min}) in native gA and RR channels were obtained in the thickest bilayers (GM-C_{20}/decane, ■, GM-C_{22}/hexadecane, ▼). For the SS channel, however, g_H^{min} values were systematically obtained in GM-C_{20}/hexadecane (□, see Fig. 9 below and Discussion), followed by measurements in the thinnest bilayers (GM-C_{16}/hexadecane, △; GM-C_{18}/hexadecane, ○; or GM-C_{18}/squalene, ◇). Proton transfer in the SS channel in relation to native gA and RR channels is differentially modulated by bilayer thickness.
3. Fig. 7 shows that g_H values in the SS channel at a given $[H^+]$ were considerably more spread out than in native gA or RR channels. The dependence of proton transfer on monoglyceride bilayer thickness was the largest in SS channels. The ratios between g_H^{max} and g_H^{min} at a given $[H^+]$ were in the range of 1.3–3.7 (SS), 1.2–1.9 (native gA), and 1.1–1.6 (RR) for various $[H^+]$.

In Fig. 8, g_H values at 0.25 M in native gA (*circles*), SS (*squares*), and RR channels (*triangles*) were plotted as a function of bilayer thickness. The concentration of 0.25 M was chosen for this plot because the difference between g_H values in the SS and native gA channels is largest in thick bilayers at that concentration (see Fig. 5, *left column*). It is shown that for the SS channel there was a significant enhancement of g_H in monoglyceride bilayers whose thicknesses were ≥ 37 Å. In gA and RR channels, changes in g_H were smaller, but definitely in the opposite direction of the SS. Significant attenuations of g_H in GM-C_{20} (with either decane or hexadecane) bilayers for the SS channels, and in GM-C_{20}/hexadecane for gA channels were measured (Fig. 8). It is likely that GM-C_{20} has a thickness-independent effect on the conformation of native gA and SS channels that disfavors proton transfer. At this point not much can be added to this observation.

It has been shown that within the range of 1 M $< [H^+] <$ 5 M, g_H saturates in the SS channel (Cukierman et al., 1997; Cukierman, 2000; Godoy and Cukierman, 2001). At these high $[H^+]$ levels, these observations also apply to bilayers with various thicknesses (Figs. 5 and 7). For the SS channel

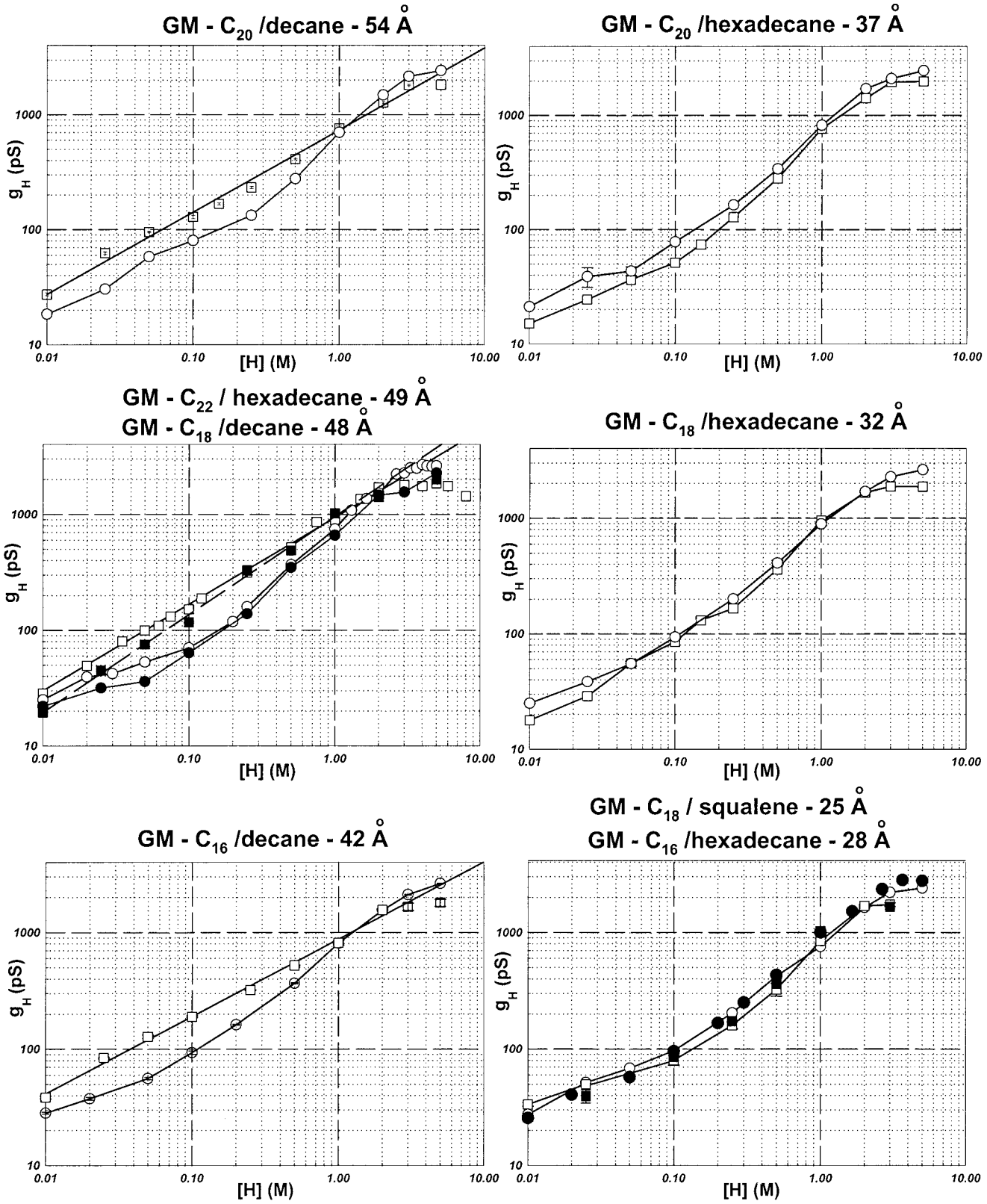

FIGURE 5 Relationships between $\log(g_H)$ and $\log([H^+])$ in monoglyceride bilayers with various thicknesses. Squares and circles represent measurements of the SS and gA channels, respectively. The type of bilayer and its thickness are indicated at the top of each panel. The solid symbols in the middle panel (*left column*), and in the bottom panel (*right column*) were obtained in GM-C_{22}/hexadecane, and in GM-C_{18}/squalene bilayers, respectively. The slopes (and linear regression coefficients) for the straight lines in the graphs of the left column were: 0.71 (0.99, *top panel*); 0.85 (1.00) and 0.75 (1.00) for the solid and open squares, respectively (*middle panel*); 0.66 (1.00, *bottom panel*).

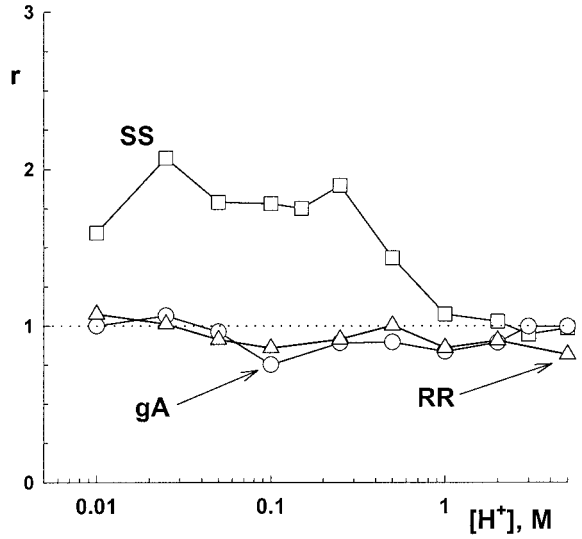

FIGURE 6 Ratios (r) between g_H values in GM-C_{18}/decane and GM-C_{18}/hexadecane in the various gA channels as a function of $[H^+]$.

in various bilayers, g_H saturated at values less than 2000 pS. For native gA channels, however, maximum g_H values were close to 3000 pS, and saturated at larger $[H^+]$ than for the SS channel (Figs. 5 and 7).

So far, the thickness of the bilayer has been considered as the independent variable, and one of the differences between thick and thin bilayers concerned the solvent used (decane for thick and hexadecane for thin bilayers). The molecular environment between the monolayers in a bilayer changes with the solvent (McIntosh et al., 1980; Simon et al., 1977; White, 1978). Thus, an alternative interpretation could be that the solvent itself was modulating proton transfer in SS channels. This possibility was addressed by measuring g_H values in GM-C_{22}/hexadecane bilayers (49 Å), and comparing them to those obtained in GM-C_{18}/decane (48 Å). Another set of experiments was performed with GM-C_{18}/squalene (25 Å), in which case the experimental measurements of g_H were compared to those obtained with GM-C_{16}/hexadecane (28 Å). These four sets of measurements were plotted as solid circles (native gA channels) and squares (SS channels) in the middle graph on the left column, and bottom graph on the right column of Fig. 5, respectively.

In the middle panel of the left column in Fig. 5, the relationship between $\log(g_H)$ and $\log([H^+])$ for $[H^+] \leq 2$ M could still be represented by a straight line for the SS channel in GM-C_{22}/hexadecane bilayers (*solid squares*). However, that straight line had a slope slightly larger (0.85) than in GM-C_{18}/decane (0.75) due to a decreased g_H at $[H^+] \leq$ 0.1 M. Interestingly, this observation also applied to native gA channels. For native gA channels, there was a good agreement between g_H values in GM-C_{18}/decane and GM-C_{22}/hexadecane bilayers. Most importantly. however, is the fact that g_H values were still larger in the SS than in native gA channels. As for the comparison between g_H-$[H^+]$

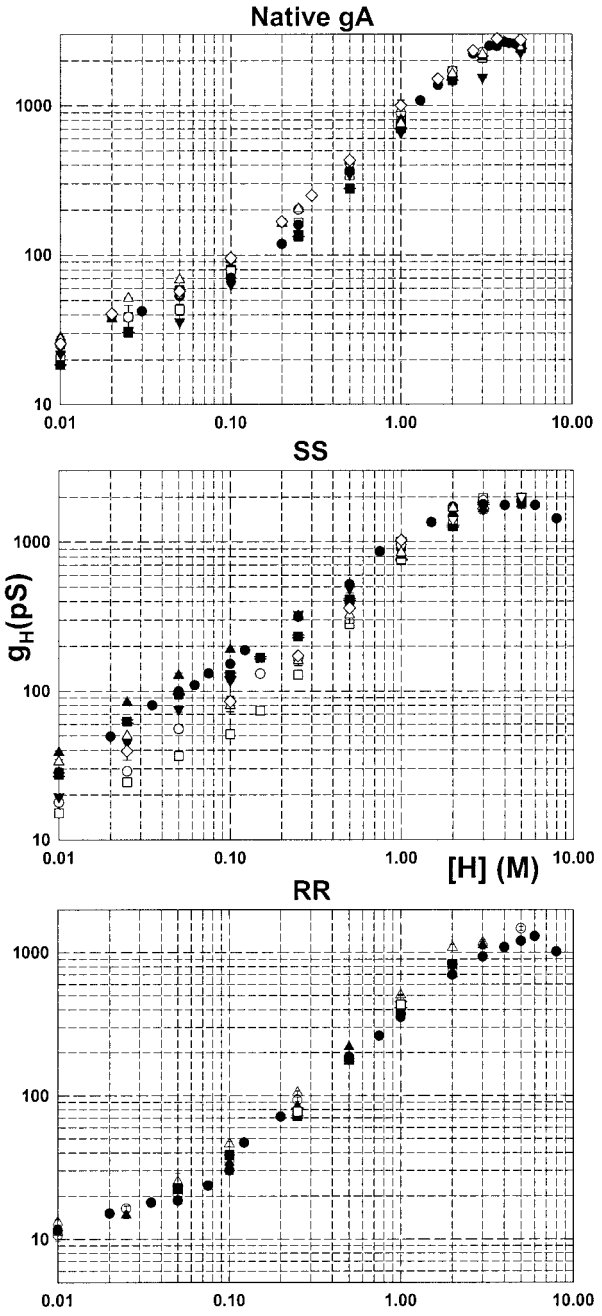

FIGURE 7 Superimposition of experimental points from Fig. 5 for the various gA channels: ■, GM-C_{20}/decane; □, GM-C_{20}/hexadecane; ●, GM-C_{18}/decane; ○, GM-C_{18}/hexadecane; ▲, GM-C_{16}/decane; △, GM-C_{16}/hexadecane; ▼, GM-C_{22}/hexadecane; and ◇, GM-C_{18}/squalene.

relationships in GM-C_{18}/squalene and GM-C_{16}/hexadecane bilayers (*bottom panel* on *right column* in Fig. 5), there was excellent agreement between the open and solid symbols (for both channels) in the log-log plots. It seems that the modulation of proton transfer in gA channels is a consequence of bilayer thickness.

Surface tension measurements at air/water interface were performed in the various lipids used in this study. No one-

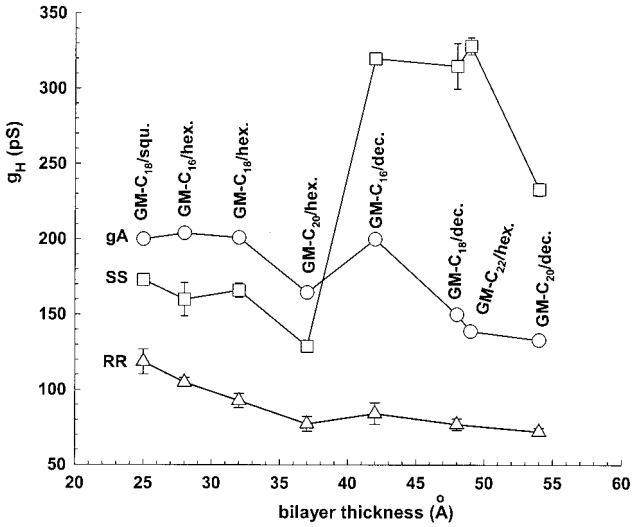

FIGURE 8 g_H vs. membrane thickness for various gA channels in 0.25 M HCl.

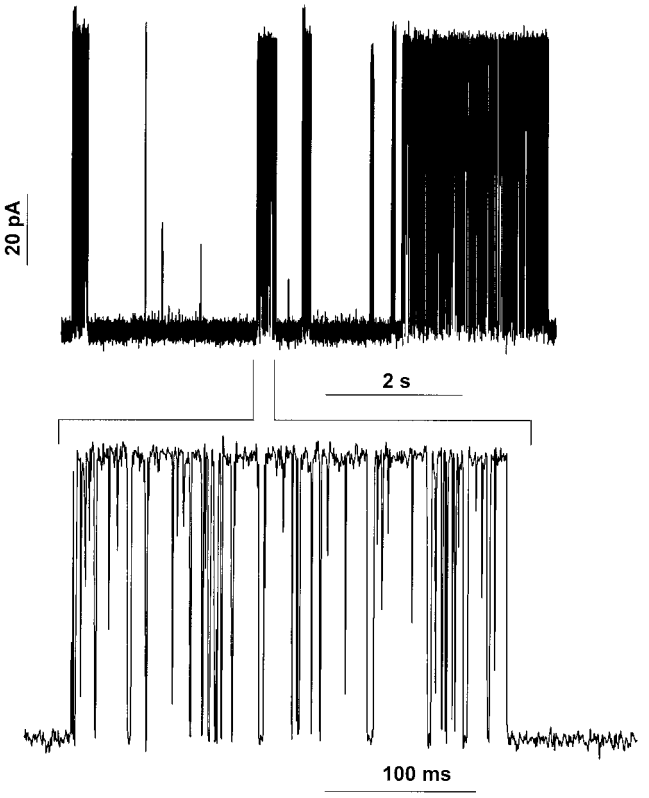

FIGURE 9 Recording of a single (likely) SS channel in a GM-C_{20}/decane bilayer (1 M HCl). The membrane voltage was 100 mV. Channel openings are represented by upward deflections of the trace. For the purpose of illustration, the original current trace (recorded at 10 kHz, and digitized at 20 kHz) was low-pass Bessel filtered at 5 kHz and the number of points of the trace was reduced 10-fold.

one relationships were found between g_H (for the various gA) and surface tension measurements (see Table 1).

The single-channel conductances to several alkalines in native gA channels seem to be independent of the thickness of the bilayer as determined by the use of various solvents (Hladky and Haydon, 1972; Kolb and Bamberg, 1977; Rudnev et al., 1981). These results contrast with g_H measurements shown above for the SS and to a more limited extent in native gA and RR channels (Figs. 5–7). In view of the conceptual importance of this issue, g_{Cs} values were measured on both the SS and native gA channels in either GM-C_{18}/decane or GM-C_{18}/hexadecane bilayers. The data in Table 2 shows that bilayer thickness (as determined by the solvent) does not have a pronounced effect on g_{Cs} on both types of channels. In 0.25 M CsCl, the ratio between g_{Cs} values in the SS channel in thick and thin bilayers is ~0.9. By contrast, the same ratio in 0.25 M HCl solutions is ~2.0 (Figs. 5 and 6).

Gating of gA channels in monoglyceride bilayers

The gating of gA channels in monoglyceride bilayers of various thicknesses followed the same pattern previously reported (Armstrong and Cukierman, 2002). As the thickness of bilayers decreased, the average lifetime of native gA channels increased (Elliot et al., 1983; Hendry et al., 1978; Hladky and Haydon, 1972; Kolb and Bamberg, 1977), and the flicker frequency in native gA (Armstrong and Cukierman, 2002; Ring, 1986; Sigworth and Shenkel, 1988), and in the SS and RR channels decreased appreciably (Armstrong and Cukierman, 2002). In particular, the inactivation of the RR channel in thick bilayers (Quigley et al., 1999) was absent in thin bilayers (Armstrong and Cukierman, 2002).

A unique observation was documented in the thickest bilayers used in this study (GM-C_{20}/decane). This is shown in Fig. 9. In GM-C_{20}/decane bilayers, it was common for both the SS and RR channels to display bursts of openings instead of very long openings (compare recordings in Figs. 3 and 9). In contrast to Fig. 3 in which the SS channel was open (with flickers) for more than 9 min, Fig. 9 shows that in GM-C_{20}/decane bilayers, the channel opens in a bursting behavior (similar to native gA channels).

TABLE 2 g_{Cs} (pS) in the SS and native gA channels

	SS		gA	
[Cs^+]	GM-C_{18}/dec.	GM-C_{18}/hexad.	GM-C_{18}/dec.	GM-C_{18} /hexad.
1 M	62.8 ± 2.3 (32)	64.7 ± 3.8 (6)	82.4 ± 0.2 (260)	84.4 ± 0.1 (175)
0.25 M	30.2 ± 1.3 (9)	33.4 ± 1.7 (13)	46.8 ± 0.1 (110)	45.1 ± 0.1 (135)

DISCUSSION

In this article, new and unsuspected characteristics of H^+ transfer in gA channels were documented. These are: *1*) Proton transfer in the SS, and to a considerably lesser extent in native gA and RR channels, is modulated by the thickness of monoglyceride bilayers. The log(g_H)-log([H^+]) plots in SS channels, which are straight lines in thick (> 37 Å) bilayers, overlap with those in native gA channels in thin bilayers. This is a consequence of a major attenuation of g_H in the SS channel in thin bilayers at [H^+] < 1 M. *2*) g_H values in native gA and RR channels are larger in the thinnest bilayers. Ratios between g_H values in thick and thin bilayers in these channels are smaller than 1 (see Fig. 6 for an example). This contrasts with the SS channels in which that ratio is considerably larger than 1. *3*) In GM-C_{20} bilayers (with either decane or hexadecane), there is a significant attenuation of g_H in native gA channels, and most notably in the SS. *4*) In monoglyceride bilayers, the saturating g_H values at high acid concentrations is consistently larger in native gA than in SS or RR channels. *5*) In the thickest bilayers used in this study, it was common for both the SS and RR channels to open in short bursts of activity.

The hydrophobic length of gA channels is ≈ 22 Å (Elliot et al., 1983). The function of gA channels (and of any membrane protein) depends on the appropriate interactions between the hydrophobic portions of gA and the membrane. In order for a gA channel to be functional in a bilayer with a hydrophobic thickness larger than 22 Å, the bilayer around the openings of a gA channel must adopt a conformation in which the openings of the channels are exposed to the outside solutions at the same time that the hydrophobic side chain residues of gA are shielded by the core of the bilayer (de Planque et al., 1998; Hendry et al., 1978; Hladky and Haydon, 1972; Helfrich and Jakobsson, 1990; Huang, 1986; Elliot et al., 1983; Killian et al., 1998; Kolb and Bamberg, 1977; Lundbæk and Andersen, 1994; Lundbæk et al., 1996; Ring, 1986; van der Wel et al., 2000). Lipid membranes are dynamical structures, and collective motions or undulations of planar lipid bilayers have been recently measured (Bayerl, 2000; Hirn et al., 1998). It is conceivable that the functionality of a native gA channel is a consequence of bilayer undulations. Two gA monomers located in opposite monolayers of a membrane will form an ion channel when thermal fluctuations in the two monolayers of the membrane bring their amino termini close enough to establish intermolecular H-bonds (see Helfrich and Jakobsson, 1990, and their Fig. 6 in particular). Consequently, ''deformations'' of the bilayer around gA channels are not static structures but the result of intrinsic dynamic fluctuations in the lipid bilayer thickness (Armstrong and Cukierman, 2002). In particular, it was proposed that undulations of the lipid bilayer underlie the fast closing flickers of various gA channels (Armstrong and Cukierman, 2002).

In a previous study, Armstrong and Cukierman (2002) have shown that proton transfer in native gA, SS, and RR channels was significantly larger in 1 M HCl in GM-C_{18}/squalene bilayers than in GM-C_{18}/decane bilayers. Considering that the resistance to proton transfer in the channel is comparable to that measured in bulk solution (Cukierman, 1999, 2000), it was reasoned that the lower g_H in thick bilayers is a consequence of the presence of significant access resistances in series with the channel. These resistances would derive from long (proportional to the difference between the thickness of bilayer and channel's length) and diffusion-restricted spaces adjacent to the mouths of the pore in thick bilayers (Armstrong and Cukierman, 2002). Although this hypothesis must be taken into consideration in attempting to explain the present experimental results, it is clear that the effects of bilayer thickness (or lipid/protein interactions) on the modulation of proton transfer in various gA channels are more complex than previously anticipated.

Proton transfer in monoglyceride bilayers

Experiments in various gA channels in [H^+] > 1 M

Previous results (Cukierman, 2000; Godoy and Cukierman, 2001) and Figs. 5 and 7 in this article demonstrated that in [H^+] > 1 M, g_H saturates. It is likely that this saturation is a consequence of diffusion limitation in bulk solution (see bottom graph in Fig. 1; also see Cukierman, 2000) at high [HCl]. As [HCl] increases, the mobility of protons in solution becomes increasingly determined by the hydrodynamic mobility of solvated H^+ instead of H^+ transfer (Agmon, 1998; Cukierman, 2000; Lengyel et al., 1962; Owen and Sweeton, 1941). This would attenuate the mobility of protons in solutions with the effect of limiting the access (exit) of protons to (from) the channel from (to) solution in concentrated acid solutions. An additional observation consistent with the mechanism described above concerns the behavior of g_H in positively charged phospholipid bilayers (Godoy and Cukierman, 2001). In those bilayers, saturation of g_H values corrected for proton concentration at the membrane/solution interface occurred at [H^+] ~0.2 M which corresponds to a $[H^+]_{bulk}$ of ~2 M. In neutral monoglyceride bilayers in 0.2 M HCl solutions (Figs. 5 and 7), g_H is still increasing with $[H^+]_{bulk}$. In relatively high [HCl], the effects of monoglyceride bilayer thickness on g_H for the various gA channels were the same as in low [HCl] (see below).

Native gA channels

Small or no changes in the single-channel conductances to alkalines in native gA channels were measured in bilayers whose thicknesses were modified by the use of distinct solvents with the same monoglyceride (Hladky and Haydon, 1972; Kolb and Bamberg, 1977). This result has been confirmed (Table 2) for g_{Cs} in GM-C_{18} with either decane

or hexadecane as the solvent. However, when the bilayer thickness was increased by using monoglycerides with longer fatty acid chains, a clear reduction in g_{Cs}, g_{Na}, and g_K (Hladky and Haydon, 1972; Kolb and Bamberg, 1977; Rudnev et al., 1981) occurred in the respective 1 M chloride solutions. These experimental results are in a sense contradictory (see below).

Whereas the shape of the $\log(g_H)$-$\log([H^+])$ plots in native gA channels was maintained in the various monoglyceride bilayers (Fig. 7, *top panel*), at a given $[H^+]$ g_H^{max} and g_H^{min} had a relatively modest (compared to SS channels), but systematic, dependence on bilayer thickness. These extreme g_H values were always measured in thin and thick monoglyceride bilayers, respectively. Contrary to previous results with alkalines (Hladky and Haydon, 1972; Kolb and Bamberg, 1977; Rudnev et al., 1981; also see Table 2) there was a clear increase in proton transfer in bilayers made thinner by using hexadecane or squalene as substitutes for decane with the same monoglyceride (see Figs. 2, 6, and 8, for specific examples). On the other hand, in GM-C_{20} bilayers, significant attenuations of g_H were measured. This is in agreement with results with alkalines (Kolb and Bamberg, 1977; Rudnev et al., 1981). In summary, in relatively thick bilayers (GM-C_{20}/decane and GM-C_{22}/hexadecane, our results; GM-C_{20}/hexadecane, Kolb and Bamberg, 1977; and GM-C_{22}/heptane, Rudnev et al., 1981) there is a general decrease in the ion-transport properties in gA channels, whereas in thin bilayers (with shorter fatty acid chains and/or by using hexadecane or squalene as solvents) there is a small but consistent increase of H^+ transfer only (Figs. 2, 5–7, and Table 2).

We now examine a few distinct possibilities (still at the qualitative level) that could account for the apparently contradictory effects of monoglyceride bilayer thickness on the single-channel conductance to protons or alkalines in native gA channels.

One possibility concerns the development of an access resistance adjacent to the mouths of the channel in thick bilayers (Armstrong and Cukierman, 2002). As discussed above, this would have the effect of attenuating g_H by increasing the access resistance to protons in thick bilayers. At relatively high alkaline concentration, the rate-limiting step for alkaline permeation resides in the channel itself (Andersen, 1983). Thus, and contrary to H^+ transfer in the channel, this access resistance is not likely to contribute significantly to the total single-channel conductance in thick or thin bilayers. Consequently, this would explain the lack of effect of bilayer thickness on the single-channel conductance to alkalines but not to g_H in native gA channels. It may well be that at low concentration of alkalines, in which diffusion limitation or access resistance plays a significant role and limits single-channel conductance (Andersen, 1983), the single-channel conductance is larger in thin than in thick bilayers. Unfortunately, the small signal-to-noise ratio for the single-channel conductances in these experimental conditions makes the investigation of this phenomenon extremely difficult.

The general decrease in the transport properties of gA channels in the thickest bilayers may result from significant alterations of the channel's structure. Therefore, a second consideration is that the overall decline of single-channel conductances in thick bilayers could reflect an increased probability of mismatch between the hydrophobic portions of channel and the thick bilayer. In thick bilayers, one or both openings of gA channels could be obliterated by the bilayer. Undulations of thick lipid bilayers could be wide enough to obliterate the openings of the channel for longer times than in thin bilayers (Armstrong and Cukierman, 2002; Bayerl, 2000; Hirn et al., 1998). Thus, the single-channel conductance to any cation in principle would represent an average value that reflects the relative times the channel spends in those conductive and nonconductive states. The fact that bursts of activity are present in dioxolane-linked gA channels (Fig. 9) provides some support to such an hypothesis. In bilayers whose thickness is $\leq$49 Å, the SS channel remains in the open state (with flickers) for tens of minutes or even hours (Cukierman et al., 1997; Quigley et al., 1999). However, in 54 Å bilayers, the SS (or RR) channels display the bursting pattern exemplified in Fig. 9. It seems reasonable to hypothesize that the intervals between bursts are a consequence of the electrical insulation of the mouths of covalently linked gA dimers from one or both solutions facing the mouths of the pore.

A third consideration is that significant fluctuations in the distance between the two gA monomers could occur in thick bilayers. These fluctuations would be a consequence of mobilities of gA monomers in monolayers in a direction perpendicular to the plane of the bilayer, and also to undulations of the membrane. Some of these gA conformations (including monomer dissociation) would disfavor ion permeation or proton transfer in the water wire in the channel, and as a consequence, single-channel conductances would be attenuated in general. In thin bilayers, fluctuations in gA intermonomeric distance would be more constrained favoring interactions that facilitate ion permeation or proton transfer. Because the transfer of protons in gA channels occurs with a time scale of 1–2 orders of magnitude faster than the permeation of alkalines (Grotthuss mechanism vs. hydrodynamic diffusion of water and alkalines), it is possible that such fluctuations would be more influential on proton transfer than on alkaline permeation. This could also explain why bilayers thinner than GM-C_{18}/decane bilayers have a small or no effect on alkaline permeation but a significant effect on proton transfer.

RR- and SS-dioxolane-linked gA channels

The influence of monoglyceride bilayer thickness on proton transfer in RR channels is qualitatively the same as in native gA channels: the shoulder shape of the log-log plots is

maintained in monoglyceride bilayers with various thicknesses, and g_H varies inversely with bilayer thickness. Thus, most of the discussion above in the context of native gA channels could also apply to RR channels. It should be remarked, though, that as in our previous studies, g_H values in the RR channel are systematically and significantly lower than in gA (or SS) channels.

Perhaps the most interesting and completely unexpected observation in this study was that g_H in SS channels is considerably larger in thick (>37 Å) than in thin monoglyceride bilayers. This occurs more dramatically in $[H^+] < 1$ M, and causes the linearization (slope <1) in the log(g_H)-log[H^+] plots. This effect was not measured with g_{Cs} (Table 2), and provides an interesting contrast to the experimental observations with the RR channel. Consequently, the enhancement of g_H in thick bilayers cannot be related to the presence of the dioxolane linker per se.

In view of some recent findings in other laboratories and our experimental results in this study, it is of interest to address some experimental factors that regulate the linear vs. nonlinear behavior in log-log plots of g_H vs. [H^+] in gA channels.

Cukierman (2000) demonstrated that not only g_H values in the SS and RR channels have different magnitudes, but the shapes of the relationships between g_H and [H^+] were also distinct (Fig. 1). The shape of the log-log relationship between g_H and [H^+] in RR channels was similar to native gA channels (Eisenman et al., 1980; Gowen et al., 2002). This can be interpreted as if two (or more) H^+ can simultaneously occupy the pore of RR channels (Hille and Schwarz, 1978). However, this idea is not immediately evident or applicable for the SS channel, which has a linear (with slopes considerably less than 1.00) log-log relationship in thick monoglyceride bilayers over a wide range of proton concentrations. We have performed calculations on the dependence of g_H on [H^+] (results not shown) using Eyring rate theory (Eyring et al., 1949; Hille and Schwarz, 1978). The model for proton permeation inside the channel consisted of a sequence of three energy peaks separated by two wells. Allowance was given for double occupancy of the pore by protons. Calculations were performed with the energy peaks and valleys located at various electrical distances inside the channel. Using this model, it was not difficult to obtain log(g_H)-log([H^+]) linear relationships with a slope of 1.00 (see, for example, Fig. 3 in Hille and Schwarz, 1978). However, linear relationships with slopes less than 1.00 in the log-log plots were not obtained. We have previously argued that the linear log-log plot in the SS channel could be a consequence of a rate-limiting step for H^+ transfer in the solution/channel interfaces (Cukierman, 2000) or inside the channel itself (Godoy and Cukierman, 2001) but not to diffusion in bulk solution. We suspect that these distinct phenomena have different relative contributions to g_H at various [H^+]. Although the cause for the linearity (slope < 1) vs. nonlinearity of H^+ transfer in gA channels in log-log plots remains unknown, in this study we demonstrated that the thickness of monoglyceride bilayers is definitely one parameter involved in this phenomenon in the SS channel.

Since our original observations (Fig. 1, Cukierman, 2000), two recent publications have demonstrated that native gA channels can also display linear log–log relationships in g_H-[H^+] plots. In one of them, Rotikskaya et al. (2002) showed that this happens in diphytanoylphosphatidylcholine/decane bilayers (slope = 0.51). We have preliminarily confirmed their results, albeit with a slope of ~0.60 (Chernyshev and Cukierman, work in progress).

Gowen et al. (2002) demonstrated that the replacement of the four Trp in gA channels by Phe (gM channels) caused linearization (slope = 1) of the log(g_H)-log([H^+]) plot. This linearization in gM channels is a consequence of a decrease and increase in g_H within the [H^+] range of 2–50 mM and 100–1000 mM, respectively. In this study, the analysis of single-channel H^+ currents was restricted to the low domain of [H^+], and the marked changes in the g_H of gM channels were attributed to a combination of three factors (gM relative to gA channels): *1*) an increase in the energy of H^+ inside the channel by ~3 kcal/mol, which has the effect of causing a substantial decrease in the probability of finding the channel occupied simultaneously by two protons over a wide range of [H^+]; *2*) the exit rate of H^+ is sped up 65-fold; and *3*) the entrance rate of H^+ in the channel is voltage-dependent in the gM channel (but not in gA), and threefold slower in gM channels. These alterations were discussed in terms of electrostatic interactions between protons and the indol groups of the Trp residues (Gowen et al., 2002).

The thermodynamic and kinetic factors that may account for the linearization of log(g_H)-log([H^+]) plots in gM channels under monooccupancy conditions (Gowen et al., 2002) do not seem to apply to a similar phenomenon caused by thick monoglyceride membranes in the SS channel: *1*) the slopes of log-log plots for the SS channel are significantly smaller than 1 in thick bilayers (see also Rotikskaya et al., 2002); *2*) thick monoglyceride bilayers cause an overall increase of g_H at $[H^+] < 1$ M, an observation which contrasts with those in gM and gA channels (see above); and *3*) it does not seem likely that different electrostatic interactions occur between protons and the Trp residues in native gA, SS, and RR channels. Nevertheless, a clear differential effect of the bilayer thickness on proton transfer in $[H^+] < 1$ M was demonstrated for the SS channel.

The most prominent structural difference between the SS and RR channels is a distortion localized in the middle of the RR channel caused by an approximate 90° tilt of the RR in relation to the SS dioxolane (Quigley et al., 1999; Stankovic et al., 1989; Yu et al., 2003). Considering this localized structural difference, distinct interactions in the middle of the SS and RR channels with thick monoglyceride bilayers could in principle account for differences in H^+ transfer between these channels. Evidently, the open question concerns the atomic details of this phenomenon.

Supported, in part, by National Institutes of Health grant GM-59674.

REFERENCES

Agmon, N. 1996. Hydrogen bonds, water rotation and proton mobility. *J. Chim. Phys.* 93:1714–1736.

Agmon, N. 1998. Structure of concentrated HCl solutions. *J. Phys. Chem.* 102:192–199.

Akeson, M., and D. W. Deamer. 1991. Proton conductance by the gramicidin water wire. Model for proton conductance in the F_0F_1AT-Pases? *Biophys. J.* 60:101–109.

Andersen, O. S. 1983. Ion movement through gramicidin A channels. Single channel measurements at very high potentials. *Biophys. J.* 41:119–133.

Andersen, O. S. 1984. Gramicidin channels. *Annu. Rev. Physiol.* 46: 531–548.

Armstrong, K. M., and S. Cukierman. 2002. On the origin of closing flickers in gramicidin channels: a new hypothesis. *Biophys. J.* 82: 1329–1337.

Armstrong, K. M., E. P. Quigley, P. Quigley, D. S. Crumrine, and S. Cukierman. 2001. Covalently linked gramicidin channels: effects of linker hydrophobicity and alkaline metals on different stereoisomers. *Biophys. J.* 80:1810–1818.

Arseniev, A. S., I. L. Barsukov, V. F. Bystrov, A. L. Lonize, and Y. A. Ovchinikov. 1985. Proton NMR study of gramicidin A transmembrane ion channel: head-to-head right-handed, single-stranded helices. *FEBS Lett.* 186:168–174.

Baciou, L., and H. Michel. 1995. Interruption of the water chain in the reaction center from *r. sphaeroides* reduces the rate of the proton uptake and of the second electron transfer to Q_B. *Biochemistry*. 34:7967–7972.

Bamberg, E., and K. Janko. 1977. The action of a carbonsuboxide dimerized gramicidin A on lipid bilayer membranes. *Biochem. Biophys. Acta.* 465:486–499.

Bayerl, T. M. 2000. Collective membrane motions. *Curr. Opinion Coll. Interf. Sci.* 5:232–236.

Benz, R., O. Frohlich, P. Lauger, and M. Montal. 1975. Electrical capacity of black lipid films and of lipid bilayers made from monolayers. *Biochem. Biophys. Acta.* 394:323–334.

Bernal, J. D., and R. H. Fowler. 1933. A theory of water and ionic solution, with particular reference to hydrogen and hydroxyl ions. *J. Chem. Phys.* 1:515–548.

Branden, M., H. Sigurdson, A. Namslauer, R. B. Gennis, P. Adelroth, and P. Brzezinski. 2001. On the role of the K-proton transfer pathway in cytochrome *c* oxidase. *Proc. Natl. Acad. Sci. USA*. 98:5013–5018.

Busath, D. D., and G. Szabo. 1988. Permeation and characteristics of gramicidin conformers. *Biophys. J.* 53:697–707.

Chernyshev, A., and S. Cukierman. 2002. Thermodynamic view of activation energies of proton transfer in various gramicidin A channels. *Biophys. J.* 82:182–192.

Chernyshev, A., R. Pomès, and S. Cukierman. 2003. Kinetic isotope effects of proton transfer in aqueous and methanol containing solutions, and in gramicidin channels. *Biophys. Chem.* In press.

Conway, B. E., J. O. M. Bockris, and H. Linton. 1956. Proton conductance and the existence of the H_3O^+ ion. *J. Chem. Phys.* 24:834–852.

Cukierman, S. 1999. Flying protons in linked gramicidin A channels. *Isr. J. Chem.* 39:419–426.

Cukierman, S. 2000. Proton mobilities in water and in different stereoisomers of covalently linked gramicidin A channels. *Biophys. J.* 78:1825–1834.

Cukierman, S., E. P. Quigley, and D. S. Crumrine. 1997. Proton Conduction in gramicidin A and in its dioxolane-linked dimer in different lipid bilayers. *Biophys. J.* 73:2489–2502.

Danneel, V. H. 1905. Notiz über ionengeschwindigkeiten. *Z. Elektrochem.* 11:249–252.

Day, T. J. F., U. W. Schmitt, and G. A. Voth. 2000. The mechanism of hydrated proton transfer in water. *J. Am. Chem. Soc.* 122:12027–12028.

De Planque, M. R. R., D. V. Greathouse, R. E. Koeppe II, H. Schäfer, D. Marsh, and J. A. Killian. 1998. Influence of lipid/peptide hydrophobic mismatch on the thickness of diacylphosphatidylcholine bilayers. A ^{2}H NMR and ESR using designed transmembrane α-helical peptides and gramicidin A. *Biochemistry*. 37:9333–9345.

DeCoursey, T. E., and V. V. Cherny. 1994. Voltage-activated hydrogen ion currents. *J. Membr. Biol.* 141:203–223.

DeCoursey, T. E., and V. V. Cherny. 1998. Temperature dependence of voltage-gated H^+ currents in human neutrophils, rat alveolar epithelial cells, and mammalian phagocytes. *J. Gen. Physiol.* 112:503–522.

Dilger, J. P. 1981. The thickness of monoolein lipid bilayers as determined from reflectance measurements. *Biochim. Biophys. Acta.* 645:357–363.

Dilger, J. P., and R. Benz. 1985. Optical and electrical properties of thin monoolein bilayers. 1985. *J. Membr. Biol.* 85:181–189.

Eisenman, G., B. Enos, J. Hägglund, and J. Sandblom. 1980. Gramicidin A as an example of a single filing ionic channel. *Ann. N. Y. Acad. Sci.* 329:8–20.

Elliot, J. R., D. Neddham, J. P. Dilger, and D. A. Haydon. 1983. The effects of bilayer thickness and tension on gramicidin single-channel lifetime. *Biochim. Biophys. Acta.* 735:95–103.

Eyring, H., R. Lumry, and J. W. Woodbury. 1949. Some applications of modern rate theory to physiological systems. *Rec. Chem. Prog.* 10: 100–114.

Finkelstein, A. 1987. Water Movement Through Lipid Bilayers, Pores, and Plasma Membrane. Theory and Reality. John Wiley & Sons, New York.

Godoy, C. M. G., and S. Cukierman. 2001. Modulation of proton transfer in the water wire of dioxolane-linked gramicidin channels by lipid membranes. *Biophys. J.* 81:1430–1438.

Gowen, J. A., J. C. Markham, S. E. Morrison, T. A. Cross, D. D. Busath, E. J. Mapes, and M. F. Schumaker. 2002. The role of *Trp* side chains in tuning single proton conduction through gramicidin channels. *Biophys. J.* 83:880–898.

Helfrich, P., and E. Jakobsson. 1990. Calculation of deformation energies and conformations in lipid membranes containing gramicidin channels. *Biophys. J.* 57:1075–1084.

Hendry, B. M., B. W. Urban, and D. A. Haydon. 1978. The blockage of the electrical conductance in a pore-containing membrane by the n-alkanes. *Biochim. Biophys. Acta.* 513:106–116.

Hille, B., and W. Schwarz. 1978. Potassium channels as multi-ion single-file pores. *J. Gen. Physiol.* 72:409–442.

Hirn, R., T. M. Bayerl, J. O. Radler, and E. Sackmann. 1998. Collective membrane motions of high and low amplitude, studied by dynamic light scattering and micro-interferometry. *Faraday Disc.* 111:17–30.

Hladky, S. B., and D. A. Haydon. 1972. Ion transfer across lipid membranes in the presence of gramicidin A. I. Studies of the unit conductance channel. *Biochem. Biophys. Acta.* 274:294–312.

Huang, H. W. 1986. Deformation free energy of bilayer membrane and its effect on gramicidin channel lifetime. *Biophys. J.* 50:1061–1070.

Ketchem, R. R., W. Hu, and T. A. Cross. 1993. High resolution of gramicidin A in a lipid bilayer by solid-state NMR. *Science*. 261:1457–1460.

Ketchem, R. R., B. Roux, and T. A. Cross. 1997. High-resolution polypeptide structure in a lamellar phase lipid environment from solid state NMR derived constraints. *Structure*. 5:1655–1669.

Killian, J. A., M. R. R. de Planque, P. C. A. van der Wel, I. Salemink, B. de Kruijff, D. V. Greathouse, and R. E. Koeppe, Ii. 1998. Modulation of membrane structure and function by hydrophobic mismatch between protein and lipids. *Pure Appl. Chem.* 70:75–82.

Koeppe II, R. E., and O. S. Andersen. 1996. Engineering the gramicidin channel. *Annu. Rev. Biophys. Biomol. Struct.* 25:231–258.

Kolb, H. A., and E. Bamberg. 1977. Influence of membrane thickness and ion concentration on the properties of the gramicidin A channel. *Biochim. Biophys. Acta.* 464:127–141.

Lengyel, S., J. Giber, and J. Tamás. 1962. Determination of ionic mobilities in aqueous hydrochloric acid solutions of different concentration at various temperatures. *Acta Chim. Hung*. 32:429–436.

Levitt, D. G., S. R. Elias, and J. M. Hautman. 1978. Number of water molecules coupled to the transport of sodium, potassium, and hydrogen ions via gramicidin nonactin or valinomycin. *Biochem. Biophys. Acta*. 512:436–451.

Lewis, B. A., and D. M. Engelman. 1983. Lipid bilayer thickness varies linearly with acyl chain length in fluid phosphatidylcholine vesicles. *J. Mol. Biol*. 166:211–217.

Luecke, H., B. Schobert, H. T. Richter, J. P. Cartailler, and J. K. Lanyi. 1999. Structure of bacteriorhodopsin at 1.55 Å resolution. *Proc. Natl. Acad. Sci. USA*. 291:899–911.

Lundbæk, J. A., and O. S. Andersen. 1994. Lysophospholipids modulate channel function by altering the mechanical properties of lipid bilayers. *J. Gen. Physiol*. 104:645–673.

Lundbæk, J. A., P. Birn, J. Girshman, A. J. Hanse, and O. S. Andersen. 1996. Membrane stiffness and channel function. *Biochemistry*. 35: 3825–3830.

McIntosh, T. J., S. A. Simon, and R. C. MacDonald. 1980. The organization of n-alkanes in lipid bilayers. *Biochim. Biophys. Acta*. 597:445–463.

Myers, V. B., and D. A. Haydon. 1972. Ion transfer across lipid membranes in the presence of gramicidin A. *Biochem. Biophys. Acta*. 274:313–322.

Nagle, J. F., and H. J. Morowitz. 1978. Molecular mechanisms for proton transport in membranes. *Proc. Natl. Acad. Sci. USA*. 75:298–302.

Nagle, J. F., and S. Tristam-Nagle. 1983. Hydrogen bonded chain mechanisms for proton conduction and proton pumping. *J. Membr. Biol*. 74:1–14.

Owen, B. B., and F. H. Sweeton. 1941. The conductance of hydrochloric acid in aqueous solutions from 5° to 65°. *J. Am. Chem. Soc*. 63:2811–2817.

Phillips, L. R., C. D. Cole, R. J. Hendershoot, M. Cotten, T. A. Cross, and D. D. Busath. 1999. Non-contact dipole effects on channel permeation. III. Anomalous proton conductance effects in gramicidin. *Biophys. J*. 77:2492–2501.

Pomès, R., and B. Roux. 1996. Structure and dynamics of a proton wire: a theoretical study of H^+ translocation along the single-file water chain in the gramicidin A channel. *Biophys. J*. 71:19–39.

Pomès, R., and B. Roux. 1998. Free energy profiles for H^+ conduction along hydrogen-bonded chains of water molecules. *Biophys. J*. 75: 33–40.

Quigley, E. P., D. S. Crumrine, and S. Cukierman. 2000. gating and permeation in ion channels formed by gramicidin A and its dioxolane-linked dimer in Na^+ and Cs^+ solutions. 2000. *J. Membr. Biol*. 174:207–212.

Quigley, E. P., P. Quigley, D. S. Crumrine, and S. Cukierman. 1999. The conduction of protons in different stereoisomers of dioxolane-linked gramicidin A channels. *Biophys. J*. 77:2479–2491.

Requena, J., D. F. Billett, and D. A. Haydon. 1975. Van der Waals forces in oil-water systems from the study of thin lipid films. *Proc. R. Soc. A*. 347:141–159.

Ring, A. 1986. Brief closures of gramicidin A channels in lipid bilayer membranes. *Biochim. Biophys. Acta*. 856:646–653.

Rotikskaya, T. I., E. A. Kotova, and Y. N. Antonenko. 2002. Membrane dipole potential modulates proton conductance through gramicidin channel: movement of negative ionic defects inside the channel. *Biophys. J*. 82:865–873.

Rudnev, V. S., L. N. Ermishkin, L. A. Fonina, and Y. G. Rovin. 1981. The dependence of the conductance and lifetime of gramicidin channels on the thickness and tension of lipid bilayers. *Bioch. Biophys. Acta*. 642:196–202.

Sarges, R., and B. Witkopf. 1965. V. The structure of valine- and isoleucine-gramicidin A. *J. Am. Chem. Soc*. 87:2011–2019.

Sass, H. J., G. Buldt, R. Gassenich, D. Hehn, D. Neff, R. Schlesinger, J. Berendzen, and P. Ormos. 2000. Structural alterations for proton translocation in the M state of wild-type bacteriorhodopsin. *Nature*. 406:649–653.

Sigworth, F. J., and S. Shenkel. 1988. Rapid gating events and current fluctuation in gramicidin A channels. *Curr. Top. Memb. Transp*. 33:113–130.

Simon, S. A., L. J. Lis, R. C. MacDonald, and J. W. Kauffman. 1977. The noneffect of a large linear hydrocarbon, squalene, on the phosphatidylcholine packing structure. *Biophys. J*. 19:83–90.

Stankovic, C. J., S. H. Heinemann, J. M. Delfino, F. J. Sigworth, and S. L. Schreiber. 1989. Transmembrane channels based on tartaric acid-gramicidin A hybrids. *Science*. 244:813–817.

Tredgold, R. H., and R. Jones. 1979. A study of gramicidin using deuterium oxide. *Biochim. Biophys. Acta*. 550:543–545.

Trumpower, B. L., and R. B. Gennis. 1994. Energy transduction by cytochrome complexes in mitochondrial and bacterial respiration: the enzymology of coupling electron transfer reactions to transmembrane proton translocation. *Annu. Rev. Biochem*. 63:675–716.

Urry, D. W. 1971. Gramicidin A transmembrane channel: a proposed $\pi_{(L,D)}$ helix. *Proc. Natl. Acad. Sci. USA*. 68:672–676.

Urry, D. W., M. C. Goodall, J. D. Glickson, and D. F. Meyers. 1971. The gramicidin A transmembrane channel: characteristics of head-to-head dimerized $\pi_{(L,D)}$ helices. *Proc. Natl. Acad. Sci. USA*. 68:1907–1911.

Van der Wel, P. C. A., T. Pott, S. Morein, D. V. Greathouse, R. Koeppe II, and J. A. Killian. 2000. Tryptophan-anchored transmembrane peptides promote formation of nonlamellar phases in phosphatydylethanolamine model membranes in a mismatch-dependent manner. *Biochemistry*. 39:3124–3133.

White, S. H. 1978. Formation of 'solvent-free' black lipid bilayer membranes from glyceryl monooleate dispersed in squalene. *Biophys. J*. 33:237–247.

Yu C. H., S. Cukierman, and R. Pomès. 2003. Theoretical study of the structure and dynamic fluctuations of dioxolane-linked gramicidin channels. *Biophys. J*. In press.

Zaslavsky, D., and R. B. Gennis. 1998. Substitution of lysine-362 in a putative proton-conducting channel in the cytochrome *c* oxidase from *Rhodobacter sphaeroides* blocks turnover with O_2 but not with H_2O_2. *Biochemistry*. 37:3062–3067.